

COMPARATIVE STUDIES ON MULTI-STORIED R.C BUILDING AND STEEL BUILDING SUBJECTED TO BLAST LOADING

K N Vishwanath ¹, M K Harikeerthan ², Ravi Kumar H ³, K V R Prasad ⁴ and Srishaila.J.M ⁵

¹ Professor And HOD, Civil Engineering Department, Dayananda Sagar Academy of Technology and Management, Kanakapura Main Road Bengaluru 560082

²Associate Professor , Civil Engineering Department, Dayananda Sagar Academy of Technology and Management, Kanakapura Main Road Bengaluru 560082

³Associate Professor & HOD, Dept of Civil Engineering, Sir M Visvesvaraya Institute of Technology, Hunasamaranahalli, Bengaluru -562157

⁴Associate Professor, Dept of Civil Engineering, Sir M Visvesvaraya Institute of Technology, Hunasamaranahalli, Bengaluru -562157

⁵ Professor and HOD, Department of Civil Engineering, S J M Institute of Technology Chitradurga -577502

Abstract— In the present study, analytical study has been carried out to examine the performance of a typical multi storied building for two cases i.e., steel building and R.C building under blast loading. For both Steel and R.C.C constructions, an eleven-storey building with plan dimensions of 25m X 20m and each storey height of 3m was considered for the study. The structure had 5 bays in the X direction with a 5m bay spacing and 4 bays in the Y direction with a 5m bay spacing. The variables considered included stand-off distance (5,10 and 15m) and charge weight (0.3,0.4 and 0.5MT) for both cases. The parameters studied for these variations included Peak base shear, Peak displacement (X and Y direction) and column forces (axial, minor and major axis moment). Increase in peak base shear and peak displacement was seen with increase in charge weight in both cases. However, peak displacement reduced with increase in standoff distance from the buildings in both cases. The axial loads and moments (minor and major axis) also increased with increase in charge weight in both cases. The R.C building showed maximum axial loads and moments when compared with steel building.

Keywords: blast loading, charge weight, standoff distance, peak base shear, peak displacement.

Introduction

A structure subjected to blast load has increased in importance as a result of unintentional occurrences or natural disasters, and in recent years, blasting of structures has been carried out as a result of structures being erected in violation of laws. Terrorist assaults on various buildings across the world have resulted in the deaths of many people as well as serious damage to these structures. Terrorist attacks have raised awareness of the importance of building structures that can withstand explosives. Due to the difficulties of transporting big explosive components, vehicles

were used in the majority of significant terrorist assaults against structures as depicted in Figure 1. Detonations of explosives in and around buildings can have devastating consequences for the building's structural integrity, such as damage to the exterior and interior structural frames and wall collapse. Furthermore, the collapse of the structure may result in the loss of life. Many owners, designers, and academics have placed a high priority on preventing such incidents. The hot gases produced by an explosion fill the surrounding area, resulting in wave propagation over space that is transmitted spherically or hemi-spherically via a medium. Understanding the behaviour of high-rise buildings subjected to blast loading is critical for avoiding or controlling explosion-related damage to structures and property. Blast-resistant structures need a thorough understanding of blast phenomena, explosions, and building blast impacts.

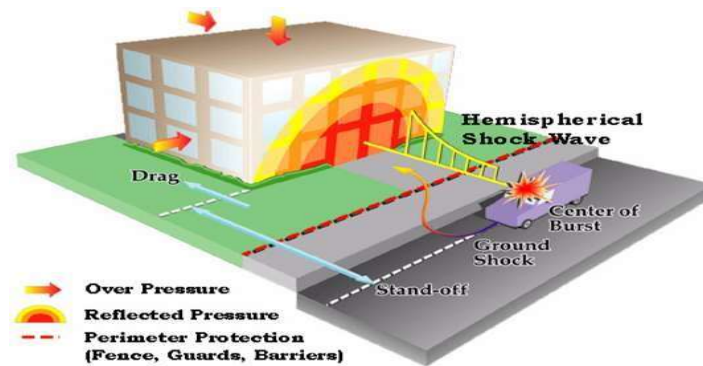


Figure 1 Blast Load on Building

A plethora of parameters govern blast loading and its implications on a structure, including charge weight, blast location (stand-off distance), R geometrical configuration, and structure orientation (or direction of blast). The structural reaction will vary depending on how these elements interact. The pressure profile can be depicted as illustrated in Figure 2 at any moment after the detonation.

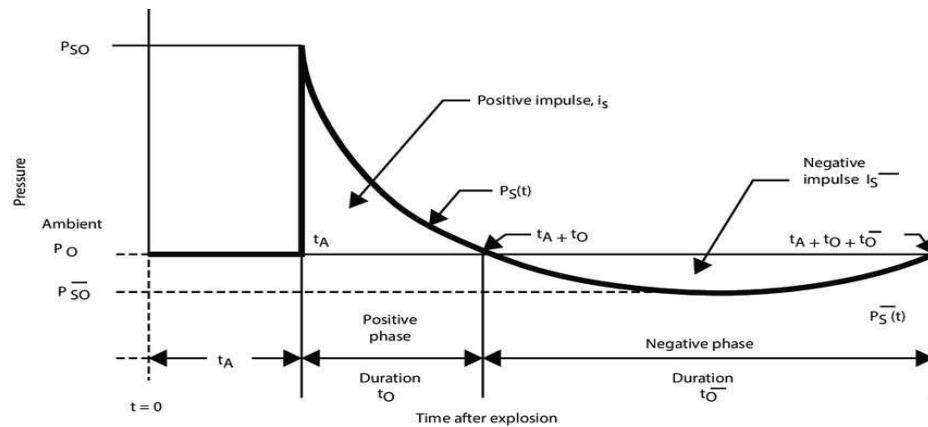


Figure 2
Characteristic
Shape of Blast Wave

As it takes time for the shock front to reach the specified location, there is no change in ambient pressure for a brief time after the detonation. The pressure rapidly climbs to that of the incident pressure at the moment of arrival, t_A , and then exponentially dissipates to the ambient pressure

conditions. The positive phase duration refers to this portion of the curve. The negative phase, which involves a suction of the air and generally lasts much longer than the positive phase, follows. The pressure will restore to ambient pressure after the negative phase is finished. Studies conducted by Kulkarni et al., (2014) examines the dynamic response of a 30-storey high rise building subjected to a blast load, as well as the principles of blast load dangers and the interaction of blast waves with buildings. SAP2000 was used for high-rise building modelling and analysis comprising of R.C. frames and infill walls. The explosive utilized was Trinitrotoluene (TNT) at two distinct standoff distances of 5m and 10m, and the model building was exposed to two different charge weights of 800lbs and 1600lbs. The blast loads are computed using the techniques described in section 5 of the TM5-1300. The behaviour of the R.C. frame and the concrete infill frame was calculated under dynamic conditions, and the dynamic load of the explosion was analyzed using a nonlinear modal analysis. This study indicated that increasing the standoff distance from the bottom floors to the upper floors has no significant influence on the upper floors owing to the lower intensity of pressure on the upper levels. Hence, increasing the standoff distance will lessen pressure on the upper floors. of the blast wave phenomena, as well as a summary of recent research on blast loads and their effects on structures. At a given standoff distance, a blast explosion within or around the structure can cause serious damage to structural and non-structural elements. The study of blast load for high-rise buildings is discussed in this work, which considers two variants of charge weights and standoff distance. Studies by Patel et al., (2017) indicate that at a given standoff distance, a blast explosion within or around the structure can cause serious damage to structural and non-structural elements. The study of blast load for high-rise buildings was also studied here which considers two variants of charge weights and standoff distance. ETABS was used to create both regular and irregular building models. The technique stated in TM 5-1300 is used to determine blast load. Based on this, the building may be made blast resistant, but not blast proof, and it is also not a cost-effective alternative due to the increased construction costs. ATBlast was also used as part of the study which estimates blast load for specified charge weights and standoff distances, and then calculates blast load dynamic characteristics such as shock front velocity, impulse, duration, and time of arrival. The increase in charge weight and decrease in standoff distance were shown to have an effect on the system. The effect of TNT (trinitrotoluene) explosive on a column foundation was examined by Unde et al., (2013) for various amounts of TNT charge weights at varied standoff distances. The blast wave characteristics for charge weights of 0.1 tonne (T), 0.2 tonne (T), 0.4 tonne (T), and 0.6 tonne (T) at 30m, 35m, and 40m standoff distances are calculated. In order to do the dynamic analysis using Staad-pro, the load is applied in the form of time history loading at nodes of beam column junctions. IS code 4991-1968 was used to compute the blast wave parameters. The results demonstrate that explosion causes significant tensile stresses in structures with fewer than six storeys. On the foundation of a structure, shear force and bending moments were also significantly reduced. Analytical investigation was carried out by Luccioni et al., (2004) using AUTODYN on the collapse of an RC building subjected to a blast load. The numerical findings are then compared to an image of real-world damage produced by an explosion. They estimated that 400 kg of TNT was planted in the building's entry hall. AUTODYN was used to simulate the columns, beams, and slabs. The results demonstrate that the numerical analysis precisely reproduces the building's collapse under blast load, verifying the explosion's position and size. Khatavkar et al (2016) studied the relevance of stand-off distance for two high-rise structures that were both closed and open (distance from the location of explosion). Blast loading was applied to RC frame constructions at distances of 0.030 km, 0.050 km, 0.070 km, 0.090 km, 0.110 km, and 0.150 km, respectively using ETABS. In

both structural situations, the minimal distance at which the structure is safe from explosion force was found out. The important factor known as Critical Distance is estimated roughly using the Von Mises stress parameter. When the highest value of Von Mises stress determined by the analysis following the application of a blast load is greater than the material's strength, the material is said to have yielded. Mishra et al., (2013) studied the behaviour of RC Framed structures during explosion. When the standoff distance is higher, blasting vibrations are lower, and when the standoff distance is smaller, blasting vibrations are greater. Finally, blasting explosive quantities should be moderately good for selection based on standoff distances in order to control blasting effect on nearby buildings. The present analytical study was taken considering the performance of high-rise RC and steel building when subjected to blast loading. Parameters such as stand off distance, charge weights were considered as part of the study. The objective of the present study are as follows

- To define pressure time history for different faces of building.
- To describe the process for estimating or generating the blast pressure time history for various blast weights (300,400 and 500kg) and standoff distances (5,10 and 15m)
- Understand the relevance of blast loading by experimenting with different charge weights and standoff distances
- Analyze and Design both Steel and R.C.C structures by linear dynamic analysis (elastic time history) subjected to blast loading.
- Comprehend the behaviour of a high-rise structure subjected to blast loading at various intensities, as well as the fluctuation of axial forces in the column.
- **Determination of the reaction of both steel and R.C.C structures in terms of base shear, displacements, and column forces, Type Style and Fonts**

Modelling AND ANALYSIS

One-dimensional frame elements for beams and columns and two-dimensional shell elements for slabs were used to create three-dimensional Steel and R.C.C structure models. Two-dimensional shell elements with six degrees of freedom at each node or one-dimensional frame elements with six degrees of freedom at both ends of the line element were considered. For both Steel and R.C.C constructions, an eleven-storey building with plan dimensions of 25m X 20m and each storey height of 3m was considered for the study. The structure had 5 bays in the X direction with a 5m bay spacing and 4 bays in the Y direction with a 5m bay spacing. For both steel and R.C.C constructions, bracings were given utilizing ISMB-250. The typical floor plan and elevation of the building is as shown in Figure 3 and Figure 4 respectively. The developed 3D model of building is assigned with all necessary material properties and sectional properties which are as shown in Figure 5.

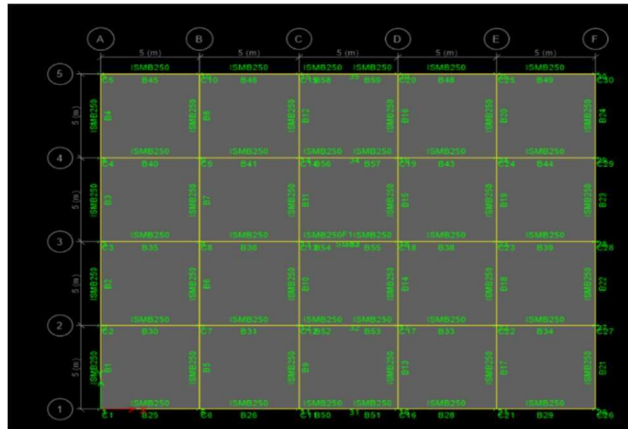


Figure 3 Typical Floor Plan with section properties

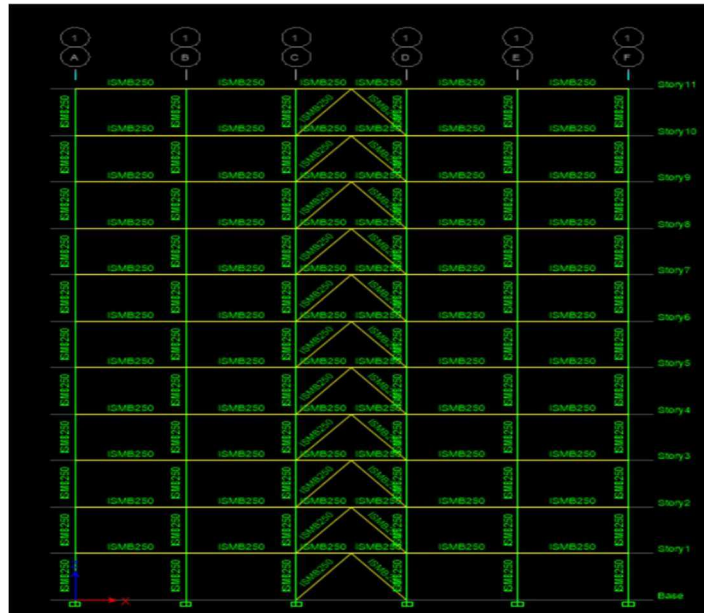


Figure 4 Typical Elevation with section properties

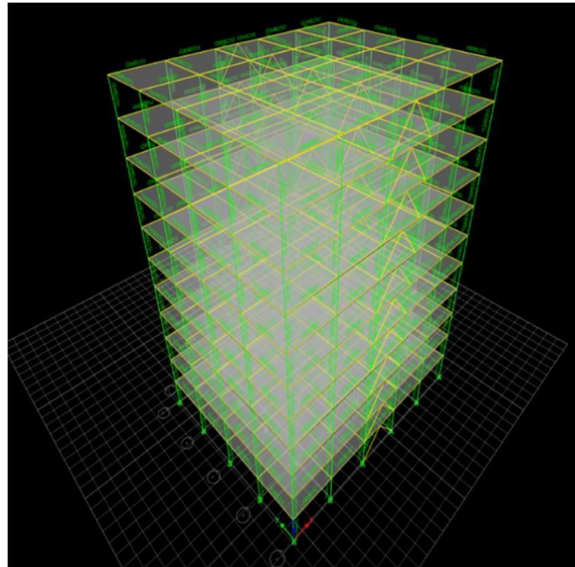


Figure 5 Typical 3D Model

RESULTS AND DISCUSSION

The purpose of this study was to determine how steel and R.C buildings respond to blast loading of three distinct intensities and standoff lengths in terms of base shear, displacements, and column forces.

STEEL STRUCTURE

The results of Blast analysis of a Steel structure is carried out for three different intensity of blast loading and three different stand-off distances using the ETABS are discussed in this section. Table 1, Table 2, Table 3 shows the base shear responses (peak) for varying charge weights (0.3, 0.4 and 0.5MT) and varying stand-off distances (5,10 and 15m). It can observed that the peak base shear increase significantly with increase in charge weight. However, the peak base shear reduces significantly with increase in stand-off distance.

Table 1 Peak Base Shear for Steel Structure in X and Y Direction for 5m Standoff Distance

Type of Model	Base Shear (kN)	
	X-Direction	Y-Direction
0.3 MT Charge weight	21153.06	2517.16
0.4 MT Charge weight	22187.71	2620.46
0.5 MT Charge weight	22916.08	2693.44

Table 2 Peak Base Shear for Steel Structure in X and Y Direction for 10m Standoff Distance

Type of Model	Base Shear (kN)	
	X-Direction	Y-Direction
0.3 MT Charge weight	9827.93	1385.82
0.4 MT Charge weight	11981.80	1601.28
0.5 MT Charge weight	13437.97	1746.57

Table 3 Peak Base Shear for Steel Structure in X and Y Direction for 15m Standoff Distance

Type of Model	Base Shear (kN)	
	X-Direction	Y-Direction
0.3 MT Charge weight	2565.76	529.66
0.4 MT Charge weight	3543.72	516.91
0.5 MT Charge weight	4637.78	850.49

Table 4, Table 5, Table 6 shows the displacements (peak) in X and Y direction for varying charge weights (0.3, 0.4 and 0.5MT) and varying stand-off distances (5,10 and 15m). It can be observed that the peak displacement increased linearly with increase in charge weight. However, the peak displacement reduced significantly with increase in stand-off distance.

Table 4 Peak Displacements for Steel Structure obtained in X and Y Direction at 5m Standoff Distance

Type of Model	Maximum Displacements (mm)	
	X-Direction	Y-Direction
0.3 MT Charge weight	21.32	14.28
0.4 MT Charge weight	28.87	17.22
0.5 MT Charge weight	41.65	21.35

Table 5 Peak Displacements for Steel Structure obtained in X and Y Direction at 10m Standoff Distance

Type of Model	Maximum Displacements (mm)	
	X-Direction	Y-Direction
0.3 MT Charge weight	13.19	6.22
0.4 MT Charge weight	14.86	8.88
0.5 MT Charge weight	17.84	9.11

Table 6 Peak Displacements for Steel Structure obtained in X and Y Direction at 15m Standoff Distance

Type of Model	Maximum Displacements (mm)	
	X-Direction	Y-Direction
0.3 MT Charge weight	7.96	3.73
0.4 MT Charge weight	10.71	5.54

0.5 MT Charge weight	13.66	6.42
----------------------	-------	------

Table 7, Table 8, Table 9 shows the results of peak column forces i.e axial load, moment variations(major and minor axis) at 5, 10 and 15m standoff distance respectively for varying charge weights (0.3,0.4 and 0.5MT)

Table 7 Peak Column Forces for Steel Structure at 5m Standoff Distance

Column	Forces	Load Case	0.3 MT weight of Charge	0.4 MT weight of Charge	0.5 MT weight of Charge
C8	Pa (kN)	BLAST (FRONT FACE)	781.37	1238.54	1934.26
	Mx (kN-m)		1.876	11.250	2.865
	My(kN-m)		2217.25	2583.40	3365.17
C14	Pa (kN)	BLAST (FRONT FACE)	518.53	957.16	1334.48
	Mx (kN-m)		2.317	19.87	1.987
	My(kN-m)		977.78	1600.82	2410.69
C21	Pa (kN)	BLAST (FRONT FACE)	65.82	215.86	332.18
	Mx (kN-m)		0.982	7.856	1.526
	My(kN-m)		2487.03	2900.64	3856.27

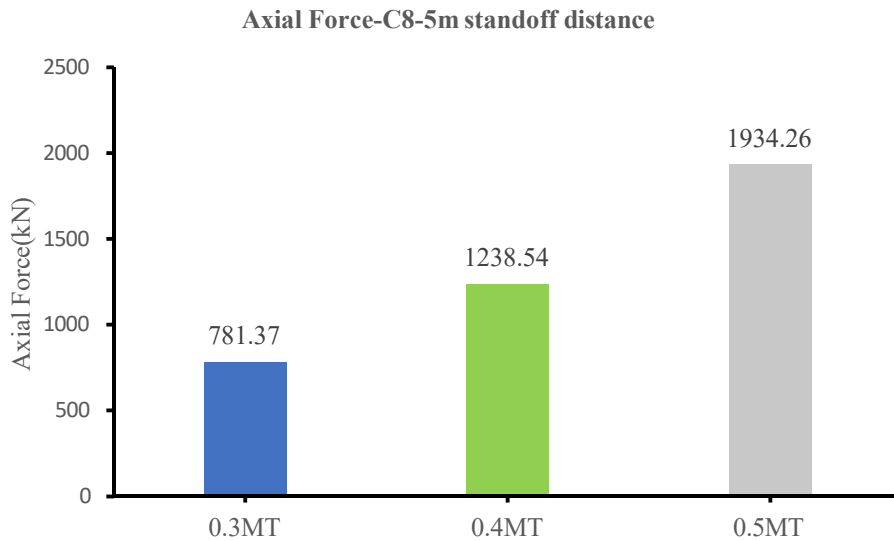


Figure 6 Variation of Axial Force- C8 column at 5m standoff distance for Steel building

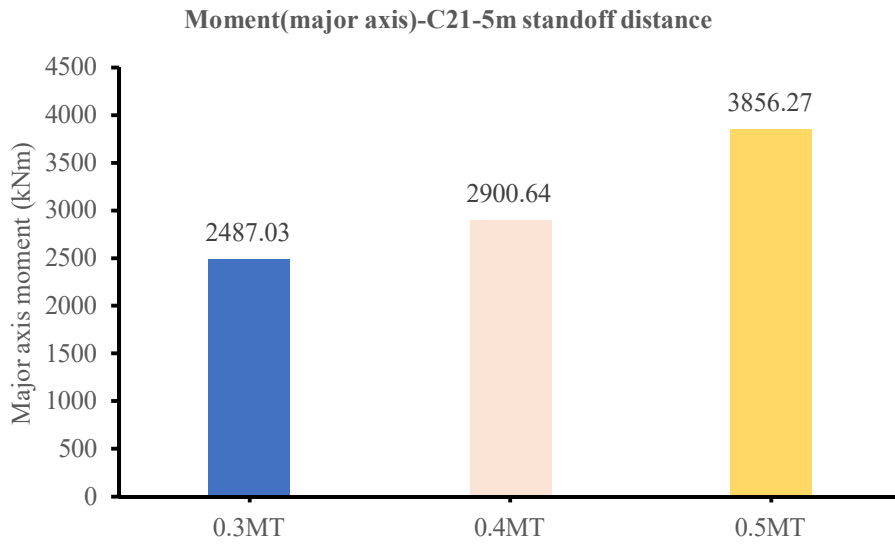


Figure 7 Variation of Major axis moment - C21 column at 5m standoff distance for Steel building

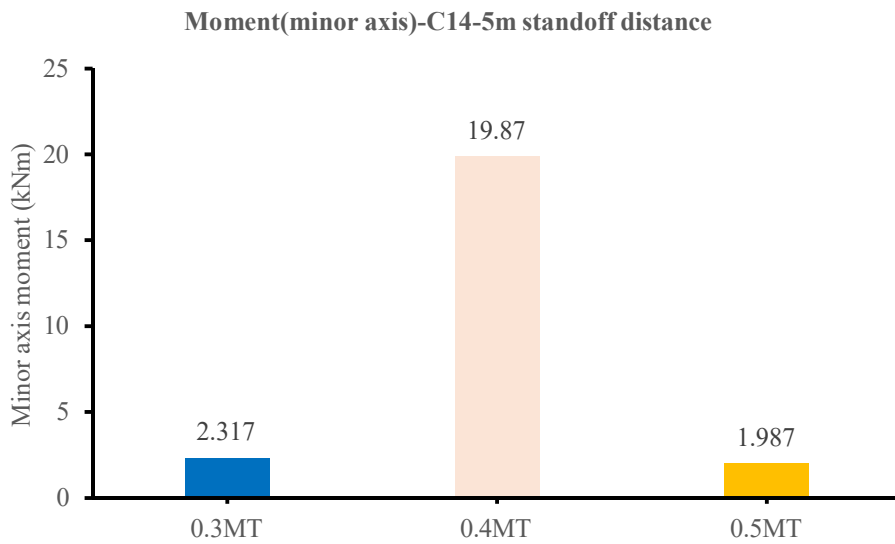


Figure 8 Variation of Minor axis moment – C14 column at 5m standoff distance for Steel building

Table 8 Peak Column Forces for Steel Structure at 10m Standoff Distance

Column	Forces	Load Case	0.3 MT weight of Charge	0.4 MT weight of Charge	0.5 MT weight of Charge
C8	Pa (kN)	BLAST (FRONT FACE)	571.21	1082.79	1722.26
	Mx (kN-m)		1.726	9.60	0.825
	My(kN-m)		1728.25	2313.07	3056.72
C14	Pa (kN)	BLAST	472.34	772.16	1117.28
	Mx (kN-m)		1.36	22.36	3.29

	My(kN-m)	(FRONT FACE)	805.22	1528.52	1632.25
C21	Pa (kN)	BLAST	116.28	347.54	497.59
	Mx (kN-m)	(FRONT	0.27	7.856	1.856
	My(kN-m)	FACE)	1903.09	2322.50	3755.38

Table 9 Peak Column Forces for Steel Structure at 15m Standoff Distance

Column	Forces	Load Case	0.3 MT weight of Charge	0.4 MT weight of Charge	0.5 MT weight of Charge
C11	Pa (kN)	BLAST	357.28	956.14	1800.17
	Mx (kN-m)	(FRONT	0.275	4.35	1.09
	My(kN-m)	FACE)	832.91	1945.81	2913.01
C14	Pa (kN)	BLAST	162.46	755.78	1163.25
	Mx (kN-m)	(FRONT	2.87	12.64	1.56
	My(kN-m)	FACE)	663.79	1224.6	2083.27
C16	Pa (kN)	BLAST	97.56	214.53	432.87
	Mx (kN-m)	(FRONT	1.94	7.23	0.88
	My(kN-m)	FACE)	1134.24	2033.41	3174.92

Maximum axial force (Pa), Major axis moment (My), and minor axis moment (Mx) in ground Story columns are sorted and summarised in Table 7, Table 8 and Table 9. The axial and major axis bending moments grew considerably, whereas the minor axis bending moment decreased after the first increase.

R.C STRUCTURE

The results of Blast analysis of R C structure are carried out for three different intensity of blast loading and three different stand-off distances using the ETABS are discussed in this section. Table 10, Table 11, Table 12 shows the base shear responses (peak) for varying charge weights (0.3, 0.4 and 0.5MT) and varying stand-off distances (5, 10 and 15m). It can be observed that the peak base shear increases significantly with increase in charge weight. However, the peak base shear reduces significantly with increase in stand-off distance.

Table 10 Peak Base Shear for R.C Structure in X and Y Direction for 5m Standoff Distance

Type of Model	Base Shear (kN)	
	X-Direction	Y-Direction
0.3 MT Charge weight	127282.06	15146.29
0.4 MT Charge weight	133507.47	15767.84
0.5 MT Charge weight	137890.51	16206.99

--	--	--

Table 11 Peak Base Shear for R.C Structure in X and Y Direction for 10m Standoff Distance

Type of Model	Base Shear (kN)	
	X-Direction	Y-Direction
0.3 MT Charge weight	59136.55	8338.75
0.4 MT Charge weight	72096.82	9635.26
0.5 MT Charge weight	80858.90	10509.84

Table 12 Peak Base Shear for R.C Structure in X and Y Direction for 15m Standoff Distance

Type of Model	Base Shear (kN)	
	X-Direction	Y-Direction
0.3 MT Charge weight	15438.68	3187.11
0.4 MT Charge weight	21323.27	3842.45
0.5 MT Charge weight	27906.46	5117.58

Table 13 Peak Displacements for R.C Structure obtained in X and Y Direction at 5m Standoff Distance

Type of Model	Maximum Displacements (mm)	
	X-Direction	Y-Direction
0.3 MT Charge weight	89.05	12.55
0.4 MT Charge weight	101.44	13.57
0.5 MT Charge weight	127.80	19.25

Table 14 Peak Displacements for R.C Structure obtained in X and Y Direction at 10m Standoff Distance

Type of Model	Maximum Displacements (mm)	
	X-Direction	Y-Direction
0.3 MT Charge weight	62.83	9.37
0.4 MT Charge weight	74.27	10.98
0.5 MT Charge weight	98.26	13.11

Table 15 Peak Displacements for R.C Structure obtained in X and Y Direction at 15m Standoff Distance

Type of Model	Maximum Displacements (mm)	
	X-Direction	Y-Direction
0.3 MT Charge weight	38.914	8.01
0.4 MT Charge weight	51.69	9.30
0.5 MT Charge weight	65.29	11.97

Table 13, 14 and Table 15 shows the maximum displacement in X and Y directions for varying charge weight (0.3,0.4 and 0.5MT) and varying standoff distance (5,10 and 15m). The maximum

displacement does get affected by the charge weight which increases linearly with increase in charge weight or blast intensity

Table 16 Peak Column Forces for R C Structure at 5m Standoff Distance

Column	Forces	Load Case	0.3 MT weight of Charge	0.4 MT weight of Charge	0.5 MT weight of Charge
C6	Pa (kN)	BLAST (FRONT FACE)	1162.74	2747.08	3688.52
	Mx (kN-m)		3.752	22.78	2.21
	My(kN-m)		4132.01	5066.24	6024.16
C11	Pa (kN)	BLAST (FRONT FACE)	937.96	1941.23	2339.86
	Mx (kN-m)		4.618	38.24	1.90
	My(kN-m)		1922.69	3201.62	4182.28
C17	Pa (kN)	BLAST (FRONT FACE)	174.25	415.39	498.07
	Mx (kN-m)		1.186	17.52	0.72
	My(kN-m)		4553.15	4875.32	7055.19

Table 17 Peak Column Forces for Steel Structure at 10m Standoff Distance

Column	Forces	Load Case	0.3 MT weight of Charge	0.4 MT weight of Charge	0.5 MT weight of Charge
C12	Pa (kN)	BLAST (FRONT FACE)	1074.42	1866.74	3421.74
	Mx (kN-m)		1.03	10.46	2.17
	My(kN-m)		3111.55	3956.01	5621.98
C15	Pa (kN)	BLAST (FRONT FACE)	821.04	1732.19	2144.22
	Mx (kN-m)		3.76	35.28	4.55
	My(kN-m)		1610.44	3056.27	3264.50
C24	Pa (kN)	BLAST (FRONT FACE)	322.56	694.08	1013.23
	Mx (kN-m)		0.46	11.245	1.48
	My(kN-m)		3706.18	4644.10	5944.23

Table 18 Peak Column Forces for Steel Structure at 10m Standoff Distance

Column	Forces	Load Case	0.3 MT weight of Charge	0.4 MT weight of Charge	0.5 MT weight of Charge
C9	Pa (kN)	BLAST (FRONT FACE)	775.83	1890.28	3411.20
	Mx (kN-m)		0.475	9.144	1.68
	My(kN-m)		1535.44	3122.47	5317.52
C15	Pa (kN)	BLAST	397.94	1511.56	2326.51

C24	Mx (kN-m)	(FRONT	3.88	15.54	2.76
	My(kN-m)	FACE)	1327.58	2049.71	3966.45
	Pa (kN)	BLAST	212.81	436.99	871.24
	Mx (kN-m)	(FRONT	1.71	11.46	0.56
	My(kN-m)	FACE)	2034.24	3933.41	5917.29

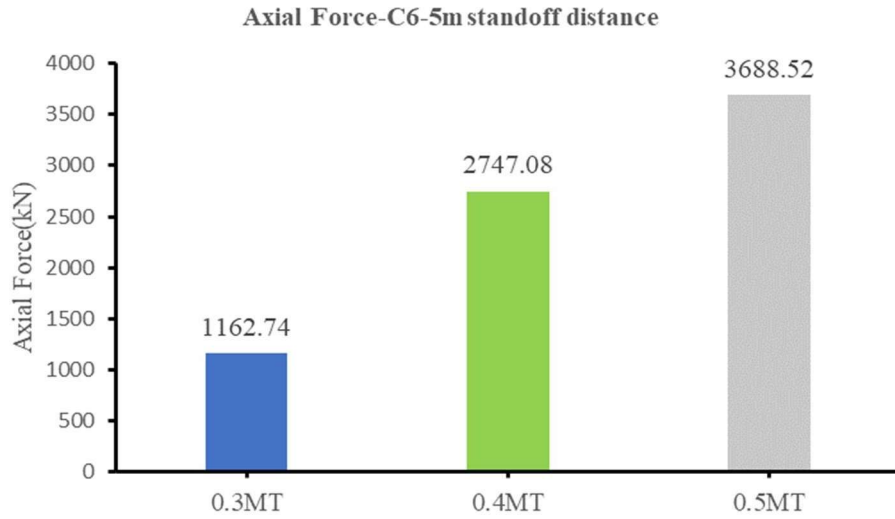


Figure 9 Variation of Axial Force- C8 column at 5m standoff distance for R.C building

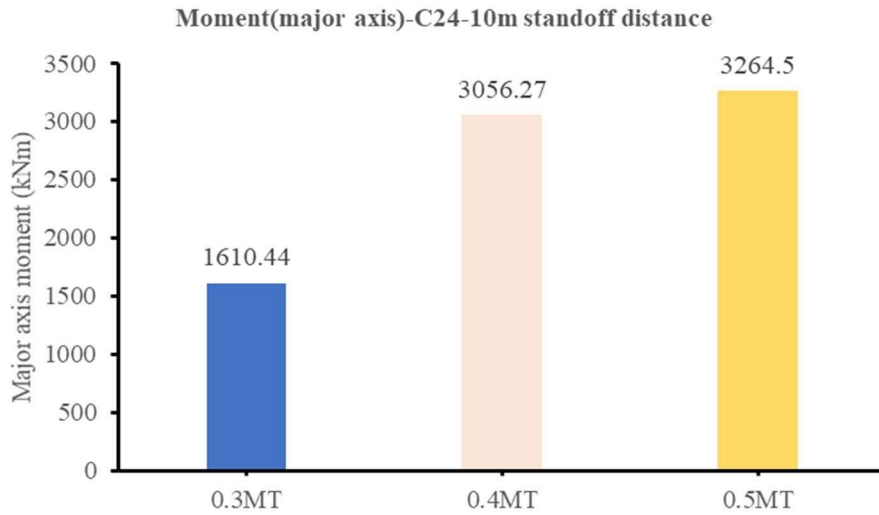


Figure 10 Variation of Axial Force- C24 column at 10m standoff distance for R.C building

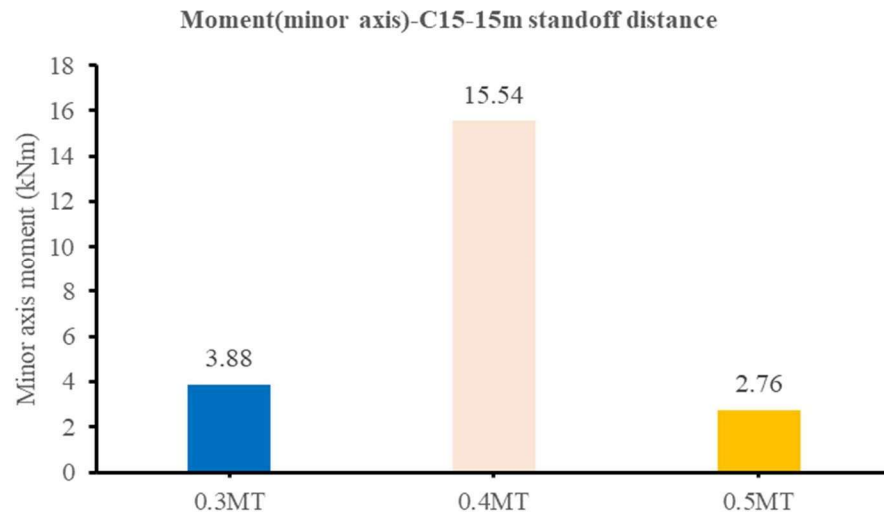


Figure 11 Variation of Axial Force- C24 column at 15m standoff distance for R.C building

Maximum axial force (Pa), Major axis moment (My), and minor axis moment (Mx) in ground Story columns are sorted and summarized above. The fluctuation of design forces in the ground floor columns is depicted in Figures 9, 10, and 11. The axial and major axis bending moments rose considerably as the blast load intensity increased, but the minor axis bending moment decreased after the first increase with the blast load intensity.

CONCLUSION

- The details of their findings are brought out in the present study. A detailed procedure of determination of blast loading for different charge weight was studied
- Analysis and design of steel and R.C.C structures is carried out using linear dynamic analysis (Elastic Time History Analysis) for the blast loading of different intensities and different standoff distances. Results of the analysis and design, are mainly maximum base shear, maximum displacement, column forces minor and major axis moments.
- The maximum base shear and the maximum displacements increased linearly as the blast loading is increased and standoff distance is decreased, the base shear causing increases the design forces of the columns and hence the displacements also increases. In the event of blast, the columns of the structure fail severely causing complete collapse.
- In blast resistant design of structures, it is very important to consider and ascertain, the blast parameters, which are justifiable, according to the standard specifications, and with reasoning of statistics and probability. Otherwise, it will lead to either 'under design' or the uneconomical design of structure.

References

1. Patil, V. B., & Sharma, A. K. (2024). Comparative performance of multi-storied RC and steel buildings under blast loads using finite element analysis. *Journal of Structural Engineering Research*, 12(4), 125–134.
2. Kumar, R., & Singh, P. (2023). Blast resistance in RC and steel structures: A parametric study. *International Journal of Advanced Civil Engineering*, 18(2), 89–101.
3. Chopra, M. R., & Das, S. (2022). Assessment of blast loading effects on RC and steel high-rise buildings. *International Journal of Structural Dynamics*, 10(3), 215–228.
4. Ahmed, H., & Al-Masri, Y. (2023). A numerical analysis of RC versus steel structures exposed to explosive forces. *Journal of Applied Structural Engineering*, 14(1), 45–56.
5. Gupta, A., & Verma, K. (2024). Influence of material properties on blast resistance of multi-storied buildings. *Civil Engineering and Materials Journal*, 22(5), 157–167.
6. Zhang, L., & Wang, Y. (2024). Comparative vulnerability of RC and steel-framed buildings to blast impacts: Experimental and simulation insights. *Journal of Engineering Mechanics*, 146(7), 1–13.
7. Sunagar, P., Nayak, S. G., & Jyothi, M. R. (2021). Analysis and Design of Water Treatment Plant Elements. *Design Engineering*, 13544-13575.
8. Sunagar, P. (2021). Seismic vulnerability and Resilience of Steel-Reinforced Concrete (SRC) and Composite Structures. *Design Engineering*, 11455-11469.
9. Sunagar, P., Kumari, T. G., Rajegowda, A. H. B., & Dharek, M. S. (2021). Innovative Design Approaches for the Seismic Response Control of Tall Buildings by Various Interior and Exterior Structural Forms. *NEW ARCH-INTERNATIONAL JOURNAL OF CONTEMPORARY ARCHITECTURE*, 8(2), 468-478.
10. Sunagar, P., Rao, K. R., Sreekeshava, K. S., Bhashyam, A., Dharek, M. S., & Nagashree, B. Analytical and Finite Element Post Buckling Analysis of Isotropic Steel Plate Subjected to the in-Plane Loading.
11. Sunagar, P., Gowda, R. S., Dharek, M. S., & Sreekeshava, K. S. Sustainable Structural Retrofitting of RC Building By Non-Linear Static Analysis.
12. Rana, A. B., Mr Shubhesh Bista, and Mr Prashant Sunagar. "Analysis of Tuned Liquid Damper (TLD) in controlling earthquake response of a building using SAP2000." *Int Res J Eng Technol* 5, no. 10 (2018): 79-96.
13. Numerical Investigations on Steel Plate Shear Walls – Stiffened and Un-stiffened by Prashant Sunagar and Priya, Publication date 2015/8, *International Journal of Innovative Research in Science, Engineering and Technology*, Volume 4, Issue 8 Pages 7156-7165
14. Blast Analysis Of A 3d Steel Frame Structure Jyothi M R, Dr. H U Raghavendra, Prashant C Sunagar, *International Journal Advanced Research Engineering a Technology (IJARET)* of in nd Volume 11, Issue 12, December 2020, pp.2518-

- 2539, article id: ijaret_11_12_238. issn print: 0976-6480 and issn online: 0976-6499
doi: 10.34218/ijaret.11.12.2020.238
15. Numerical Investigation on Concrete Shear Wall with Different Percentages of Openings, Prashant Sunagar 2015/7, International Research Journal of Engineering and Technology (IRJET), Volume 2, Issue 4, Pages 1407-1414
 16. Dynamic Response Of 3D Steel Frame, prashant Sunagar, Publication date 2014/. International Journal of Scientific & Engineering Research, Volume 5, Issue 6, ISSN 2229-5518
 17. Kannan, G. R., Vijayakumar, B., Senthil, T. S., Sunagar, P., Kumar, R. R., Parida, L., & Subbiah, R. (2022). Optimization and electro chemical grinding surface investigation on eglin steel. *Materials Today: Proceedings*.
 18. Dharek, M. S., Vengala, J., Sunagar, P., Sreekesava, K. S., Kilabanur, P., & Thejaswi, P. (2022). Biocomposites and Their Applications in Civil Engineering—An Overview. *Smart Technologies for Energy, Environment and Sustainable Development, Vol 1*, 151-165.
 19. Sunagar, P., Dharek, M. S., Nruthya, K., Sreekesava, K. S., Nagashree, B., & Ramegowda, R. S. (2020, November). Non-Linear Seismic Analysis of Steel Plate Shear Wall Subjected to Blast Loading. In *IOP Conference Series: Materials Science and Engineering (Vol. 955, No. 1, p. 012025)*. IOP Publishing.
 20. Sunagar, P., Bhashyam, A., Dharek, M. S., Sreekesava, K. S., & Rakshith, K. (2020). Instability Analysis of Fiberglass Reinforced Plastic (FRP) Subjected to the In-Plane Loading. In *Emerging Technologies for Sustainability (pp. 473-476)*. CRC Press.
 21. Nair, Avinash, S. D. Aditya, R. N. Adarsh, M. Nandan, Manish S. Dharek, B. M. Sreedhara, Sunagar C. Prashant, and K. S. Sreekesava. "Additive Manufacturing of Concrete: Challenges and opportunities." In *IOP Conference Series: Materials Science and Engineering*, vol. 814, no. 1, p. 012022. IOP Publishing, 2020.
 22. Rao, K. R., Sreekesava, K. S., Dharek, M. S., Sunagar, P. C., & Ganesh, C. R. (2020, March). Spatial variation of climate change issues using remote sensing technique. In *IOP Conference Series: Materials Science and Engineering (Vol. 814, No. 1, p. 012042)*. IOP Publishing.
 23. Sunagar, P., Bhashyam, A., Dharek, M. S., Sreekesava, K. S., Ramegowda, R. S., & Lakshmi, H. S. (2020, March). Blast resistance of steel plate shear walls designed for seismic loading. In *IOP Conference Series: Materials Science and Engineering (Vol. 814, No. 1, p. 012041)*. IOP Publishing.
 24. Sunagar, P., Bhashyam, A., Shashikant, M., Sreekesava, K. S., & Chaurasiya, A. K. (2021). Effect of Different Base Isolation Techniques in Multistoried RC Regular and Irregular Building. *Trends in Civil Engineering and Challenges for Sustainability*, 391-403.
 25. Sunagar, Prashant, Aravind Bhashyam, B. R. Neel, and Abhishek Kumar Chaurasiya. "Sustainability concepts in the design of tall structures." In *International Conference on Emerging Trends in Engineering (ICETE)*, pp. 270-277. Springer, Cham, 2020.
 26. Sunagar, P., & Shivananda, M. S. (2012, June). Evaluation of Seismic Response Modification Factors for RCC Frames by Non-Linear Analysis. In *International Conference on Advances in Architecture and Civil Engineering (pp. 322-327)*.

27. Progressive Collapse Analysis of T shape RCC Building, Prashant Sunagar¹, Shivaraj G Nayak², T G Geethakumari¹, by IOP Conference Series: Earth and Environmental Science, Volume 1125, 2nd International Conference on Sustainable Infrastructure with Smart Technology for Energy and Environmental Management (SIC-SISTEEM 2022) 24/03/2022 - 26/03/2022
28. IOT-based Solar Panel Tracking System to Enhance the Output Power, Mani P.K¹, Prashant Sunagar², Madhuri N S, Proceedings of the Third International Conference on Smart Electronics and Communication (ICOSEC2022) DVD Part Number: CFP22V90-DVD; ISBN: 978-1-6654-9763-3, 978-1-6654-9764-0/22/\$31.00 ©2022 IEEE Explore
29. Prashant Sunagar¹, Shivaraj G Nayak², Progressive Collapse Analysis of T shape RCC Building IOP Conference Series: Earth and Environmental Science, Volume 1125, 2nd International Conference on Sustainable Infrastructure with Smart Technology for Energy and Environmental Management (SIC-SISTEEM 2022) 24/03/2022 - 26/03/2022 Online, Prashant Sunagar et al 2022 IOP Conf. Ser.: Earth environ. sci. 1125 012017, doi 10.1088/1755-1315/1125/1/01201
30. B.P.R.V.S. Priyatham, S.Sivakumar, Prashant Sunagar, J. Prakash Arul Jose, “ Seismic analysis and design of steel beam-column connections in Indian standard code framework”, Materials Today: Proceedings,2023, ISSN 2214-7853, <https://doi.org/10.1016/j.matpr.2023.03.365>.
31. Ragi Krishnan, Vivek Kumar Mishra, Prashant Sunagar “Finite Element Analysis of steel frames subjected to post-earthquake fire”, Materials Today: Proceedings, 2023, ISSN = 2214-7853, <https://doi.org/10.1016/j.matpr.2023.03.671>